

Design of end-of-pipe zero liquid discharge systems under variable operating parameters

Edgard El Cham, Sabla Alnouri*, Fatima Mansour, Mahmoud Al-Hindi

Baha and Walid Bassatne Department of Chemical Engineering and Advanced Energy, American University of Beirut, Beirut, Lebanon

ARTICLE INFO

Article history:

Received 28 May 2019

Received in revised form

8 November 2019

Accepted 4 December 2019

Available online 6 December 2019

Handling Editor: Kathleen Aviso

Keywords:

Zero liquid discharge

Design

Optimization

Temperature

Salinity

Variable

ABSTRACT

Zero-liquid discharge systems have proven to be quite effective as a long-term brine management strategy. The availability of powerful modelling and optimization tools for the design of cost-effective zero-liquid discharge systems is vital, so as to ensure that only the best-performing systems are designed, constructed and operated. To date, the design of Zero Liquid discharge systems has been modelled in terms of flow rate only, without accounting for the effect of other parameters such as the feed salinity, temperature and pressure. The focus of this work is to integrate additional operating parameters (mainly temperature, salinity and electricity pricing), into a modified optimization model and to determine, more accurately, the best zero liquid discharge system configuration based on specific brine feed characteristics. The proposed model has been implemented using a case study, and sensitivity analysis is performed to determine the most optimal structure under different inlet conditions. The results indicate that the optimal configuration is highly sensitive to brine temperature and salinity. Moreover, this work also demonstrates how non-brine related conditions, such as electricity pricing, affects the design of such systems. When compared to Mansour et al. (2018), the capital costs were comparable, however, the operating costs of Zero-liquid discharge systems have been captured more effectively after introducing additional model parameters.

© 2019 Elsevier Ltd. All rights reserved.

1. Introduction

The accelerating rate of global population growth and the subsequent increase in water demand have burdened the available water resources. As such, the necessity for sustainable water sources has become a pressing matter (Subramani and Jacangelo, 2014). Desalination technologies have gained much attention in recent years as their performance and application has grown throughout the years (Morillo et al., 2014). However, brine streams pose a major challenge in terms of their disposal and the associated environmental impacts. It has been estimated that the daily brine production from desalination plants around the world is approximately 142 million m³ (Jones et al., 2019). Brine composition, volume and disposal techniques affect brine disposal cost (Morillo et al., 2014) which can constitute up to a third of total product water cost for desalination technologies (Gilron, 2016).

The selection of the optimal brine management strategy depends on several factors including brine volume and composition,

discharge location, and the capital and operating costs (Giwa et al., 2017). Surface water discharge, deep well injection and land application are common brine disposal options.

Brine reaching surface water or groundwater remains a matter of concern (Mackey and Seacord, 2008). Given the brine's composition and temperature, its disposal into water bodies endangers living organisms and marine ecosystem (Liu et al., 2018). Eutrophication, sterilization, build-up of harmful pollutants and the variation of the water pH are environmental impacts associated with brine discharge (Perez-Gonzalez et al., 2012).

As a result, the implementation of Zero Liquid Discharge (ZLD) technologies as an effective long-term alternative. These systems have witnessed technological advancements, rendering them more economically viable and leading to their application in the brine management of several industries (Subramani and Jacangelo, 2014).

ZLD refers to any process or combination of processes through which there is no liquid effluent from a chemical process plant. Existing ZLD systems focus mainly on the evaporation and crystallization processes, which are not always the optimal technologies to treat brine. ZLD is usually achieved by concentrating the

* Corresponding author.

E-mail address: sa233@aub.edu.lb (S. Alnouri).

brine stream using several processes, such as thermal and membrane-based systems, followed by a brine-to-salt processing stage for salt recovery (Ahirrao, 2014). Hence, ZLD increases the water supply while reducing water pollution, but at the expense of high cost and intensive energy consumption (Tong and Elimelech, 2016). Therefore, reliable and efficient ZLD configurations must be designed through the combination of different technologies to achieve optimal water recovery and energy consumption while accounting for the produced salt (Tillberg, 2004). It should be noted that a number of promising ZLD technologies (such as membrane distillation and forward osmosis) are currently in the research and development stage but have not been used on an industrial scale (Tsai et al., 2017; Lee et al., 2019). These technologies will not be considered in this work.

Tufa et al. (2015) proposed the use of direct contact membrane distillation together with reverse electrodialysis, to attain a near-zero liquid discharge system. Even though the proposed system was optimized by Tufa et al. (2015) for best operating conditions, the actual implementation of the design on an industrial scale was found challenging, due to the relatively limited availability of ion-exchange membranes and their high manufacturing costs. Schwantes et al. (2018) presented a technological and economic comparison between the use of membrane distillation and mechanical vapor compression in ZLD systems, and found that membrane distillation can be at least 40% more cost-effective in a ZLD system. However, they are still not commercially available for large-scale applications (Schwantes et al., 2018). Loganathan et al. (2016) conducted a pilot-scale study on the treatment of basal aquifer by using ultrafiltration, reverse osmosis and crystallization to achieve zero-liquid discharge. Lu et al. (2019) developed a mathematical model for a ZLD system that uses freeze desalination and membrane distillation-crystallization powered by solar energy and studied the effect of various parameters on its performance. Moreover, Able et al. (2018) suggested using Joule-heating desalination and flashing for the sustainable management of hypersaline brine waste resulting from oil and gas wells. Through simulation, it was found that desalination and two-stage flashing can achieve ZLD (Able et al., 2018). Additionally, Lopez and Tremblay (2017) modelled a ZLD system that consists of chemical pre-treatment combined with Joule-heating, and utilized Aspen Plus to estimate the respective economics of such systems.

Mansour et al. (2018) proposed an effective optimization approach to identify cost-effective ZLD strategies, mainly based on flowrate requirements in system. A stochastic model that assesses the design of ZLD systems under uncertainty, mainly for desalination plants, has also been proposed by (Onishi et al., 2017). It is evident that the vast majority of investigators did not account for the effect of parameters such as temperature, salinity and pressure, which often have quite an influence on the overall design cost of such systems. Thus, it was found imperative to further investigate the effects of such parameters on various ZLD system designs.

As pertains to the technology train of a complete ZLD system, specific sequences of technologies are permitted for optimal performance. This is because the brine feed can have certain components that cause the sub-par performance and fouling of the thermal and membrane systems. As such, a chemical processing stage of the brine is required to overcome these limitations and ensure optimal performance downstream. This stage is followed by a thermal based or membrane based technology(s) with salt processing technologies at the end of the system. Each stage must include various technology choices, and a selection process for which choice to use at each stage must be carried out (Mansour et al., 2018). In summary, a ZLD process for brine treatment commences with a primary stage, which usually involves the use of

chemical precipitation, or less frequently, membrane pre-treatment using NF. This stage is followed by secondary stage where thermal (e.g. MSF, MED) or membrane processes (RO) are utilized to produce a more concentrated brine and recover water. Finally, the remaining highly concentrated brine undergoes a tertiary treatment (brine-to-salt) step where processes such as crystallizers or evaporation ponds are used to achieve the zero-liquid discharge.

Mansour et al. (2018) developed a model for the ZLD network, taking into consideration various technology options at each step. The purpose of the model is to develop a cost-assessment strategy by selecting the best combination of technologies depending on specific feed conditions supplied by the user. The model focused on determining optimal flow distribution and allocation between the different technologies given that most of the data collected was a function of flow rate. Furthermore, the model was able to capture the effect and the evolution of salinity throughout the system through the incorporation of water recovery and salt rejection parameters for each processing option. As a result, the performance of various combinations of ZLD technologies could be assessed. However, the model did not take into account the effect of varying inlet conditions, such as temperature, pressure and salinity.

The improvements of the model developed in this work in comparison to the one introduced by Mansour et al. (2018) help in predicting more accurately the performance of ZLD systems by integrating temperature, pressure and salinity as variable parameters. The previous model relied solely on flow rate as an influencing parameter and thus the synthesized ZLD schemes are not as intricate as that of the developed model. Moreover, while the previous model uses fixed values for the recovery and rejection of the technologies, the developed model optimizes the recovery and calculates the rejection. Despite the availability of the information and resources required for the development of this model, the difficulty of the task lies in combining different sources of information together, in order to capture the effects of the added parameters, something that has not been attempted before.

2. Mathematical formulation

The problem formulation is expanded to incorporate the effect of additional parameters such as temperature and salinity. Its main purpose remains to develop a cost-assessment strategy that can select a combination of technologies ensuring a cost effective ZLD design according to user-specified data. Given that the cost is affected by flowrate, temperature, salinity and pressure among other variables, the main aim was to determine the optimal value for each of the mentioned parameters, and based on user-specified information, to determine the optimal ZLD configuration at the lowest cost.

2.1. Proposed modifications

The main modifications implemented to the original model (Mansour et al., 2018) are the addition of a discharge stream prior to the ZLD system and the inclusion of temperature, pressure and salinity parameters to capture their effects on the performance of the technologies.

2.1.1. Discharge stream

The discharge fraction (DF) is a user defined parameter that specifies the percentage of the feed that will not go through the ZLD system. The discharge stream (DS) is defined as follows:

$$DS = F_{in} * DF \quad (1)$$

Hence, the new feed flowrate (F'_{in}) is defined as follows:

$$F'_{in} = F_{in} - DS = F_{in}(1 - DF) \quad (2)$$

Thus, the change required to the original model is the replacement of the inlet feed flowrate with F'_{in} which accounts for the discharge stream.

2.1.2. Chemical precipitation

Lime softening is affected by the temperature at which it is carried out; a higher temperature leads to a higher removal efficiency of hardness. Thus, the chemical precipitation temperature (T_{cp}) can fall into one of three categories: cold, warm (49–60 °C) and hot (108–116 °C). Hardness must be reduced in order to ensure the smooth operation of membrane technologies by avoiding scale formation. The Langelier Saturation Index (LSI) can be used to assess the water's scaling potential; a negative value indicates that the water is non-scale forming (Kucera, 2015).

2.1.3. Thermal technologies

The thermal technologies considered in developing the model are MED and MSF. The design equations used are found in the Desalination Economic Evaluation Program (DEEP) manual (International Atomic Energy Agency, 2013).

Considering T_{cp} is the feed temperature into the technologies and T_{cr} is the distillation plant condenser range, the last stage temperature for both MED and MSF can be calculated as follows:

$$T_{therm} = T_{cr} + T_{cp} \quad (3)$$

Moreover, the plant's specific temperature range (T_{str}) is the difference between the top brine temperature (TBT) and the last stage temperature (T_{therm}), as follows:

$$T_{str} = TBT - T_{therm} \quad (4)$$

Given the minimum temperature interval of operation of each stage (ΔT_{stage}), the total number of stages required is then computed as follows:

$$n = \frac{T_{str}}{\Delta T_{stage}} \quad (5)$$

The product water (PW_t) and concentrated brine (CB_t) flowrates are a function of the feed flowrate (F_t) and the recovery (R_t), as shown below.

$$PW_t = F_t * R_t \quad (6)$$

$$CB_t = F_t * (1 - R_t) \quad (7)$$

The required electricity (Q_{et}) depends on the product water stream (PW_t) and the specific power use (Q_{sp}); it is calculated as follows:

$$Q_{et} = \frac{PW_t}{24 * 1000} * Q_{sp} \quad (8)$$

The required heat (Q_{ht}), shown below, is a function of the product water (PW_t), the gained output ratio (GOR) and the latent heat at the top brine temperature (TBT).

$$Q_{ht} = \frac{PW_t}{GOR * 24 * 3600 * 1000} * \Delta H(TBT) \quad (9)$$

2.1.3.1. MED. The GOR can be calculated in several manners (Frantz and Seifert, 2015; Gude, 2018). For the purpose of this work, the GOR is calculated as follows:

$$GOR = k_{GOR} * n \quad (10)$$

with the GOR, Q_{sp} can be calculated as follows:

$$Q_{sp} = 1.5 + 0.1(GOR - 10) \quad (11)$$

2.1.3.2. MSF. The brine heater temperature rise (T_{bh}) is a function of the specific temperature range (T_{str}), the number of stages (n) and the number of reject stages (n_r), as shown below.

$$T_{bh} = T_{str} \frac{n}{n + n_r} \quad (12)$$

The average boiling point elevation (BPE) is a function of the temperature and the composition of the feed flowrate ($x_{c,t}$), as below.

$$BPE = x_{c,t} (6.71 + 0.0634T + 0.0000974T^2) * 10^{-6} \quad (13)$$

The MSF's GOR is a function of the latent heat at the average condensing temperature (T_{ac}), the specific heat in the brine heater (c_h), the brine heater temperature rise (T_{bh}), the average boiling point elevation (BPE), the average brine specific heat capacity (c_b), the specific temperature range (T_{str}) and the latent heat at the average temperature between the top brine temperature (TBT) and the last stage temperature (T_{therm}); the relation is as follows.

$$GOR = \frac{\Delta H(T_{ac})}{C_h(T_{bh} + BPE)} \left(1 - e^{-\frac{c_b T_{str}}{\Delta H \left(\frac{TBT + T_{therm}}{2} \right)}} \right) \quad (14)$$

Consequently, Q_{sp} is calculated as follows:

$$Q_{sp} = 3.2 + 0.2(GOR - 8) \quad (15)$$

2.1.4. Membrane technologies

The DEEP reverse osmosis model has been utilized estimate the total power required (Q_{tot}) for desalination for a given feed flowrate (F_m).

The recovery (R_m) is a function of the pressure (P_m) and the composition of the membrane feed flowrate ($x_{c,m}$), as below:

Table 1

Additional and modified constraints for the new model (International Atomic Energy Agency, 2013; Eltawil et al., 2009; Mickley, 2008; Al-Karaghoulis and Kazmerski, 2013; Baghdadi et al., 2018; SaltWorksTech, n.d.).

Chemical Precipitation ^a	Langlier Saturation Index (LSI) ≤ 0
Thermal Technologies ^a	$PW_t \leq 400,000 \text{ m}^3/\text{day}$ $R_{MED} \leq 65\%$ $R_{MSF} \leq 50\%$ $x_{c,t}^{CB} \leq 360,000 \text{ mg/L}$
Membrane Technologies ^a	$PW_m \leq 400,000 \text{ m}^3/\text{day}$ $P_m \leq 82 \text{ bar}$ $T_m \leq 45 \text{ }^\circ\text{C}$
Brine Crystallizer ^a	$PW_B \leq 125 \text{ m}^3/\text{day}$

^a (International Atomic Energy Agency, 2013; Eltawil et al., 2009; Mickley, 2008; Al-Karaghoulis and Kazmerski, 2013; Baghdadi et al., 2018; SaltWorksTech, n.d.).

$$R_m = 1 - \frac{0.00115}{P_m} * x_{c,m} \tag{16}$$

The product water (PW_m) and concentrated brine (CB_m) streams are a function of the feed flowrate (F_m) and the recovery (R_m), as follows:

$$PW_m = F_m * R_m \tag{17}$$

$$CB_m = F_m(1 - R_m) \tag{18}$$

The brine stream salinity (x_{c,m}^{CB}) is calculated as follows:

$$x_{c,m}^{CB} = \frac{x_{c,m}}{1 - R_m} \tag{19}$$

On the other hand, the product water salinity (x_{c,m}^{PW}) is a function of the feed salinity (x_{c,m}), the nominal permeate flux (N_{flux}), design average permeate flux (D_{flux}), the recovery (R_m) and the membrane feed water temperature (T_m); the relation is as follows.

$$x_{c,m}^{PW} = 0.0025 * x_{c,m} * \frac{N_{flux}}{D_{flux}} * 0.5 * \left(1 + \frac{1}{1 - R_m}\right) * (1 + (T_m - 25) * 0.03) \tag{20}$$

The average pressure (P_{avg}) depends on the osmotic pressure function (Π(C,T)) and the aggregation of the individual ions correction factor (k_{agg}), as shown below.

$$P_{avg} = \frac{\Pi(x_{c,m}, T_m) + \Pi(x_{c,m}^{CB}, T_m)}{2} * k_{agg} \tag{21}$$

$$\Pi(C, T) = \frac{0.0000348(T + 273)C}{14.7} \tag{22}$$

The design net driving pressure (NDP) is a function of the design average permeate flux (D_{flux}), the nominal permeate flux (N_{flux}), the salinity correction factor (k_{sal}), the nominal net driving pressure (NDP_n), the temperature correction factor (k_{tem}) and the fouling factor (k_{fou}), as follows:

$$NDP = \frac{D_{flux}}{N_{flux} * k_{sal}} * NDP_n * \frac{k_{tem}}{k_{fou}} \tag{23}$$

The high head pump pressure rise (P_{hhp}) depends on the average pressure (P_{avg}), the net driving pressure (NDP), the pressure drop across the system (ΔP_{sys}), the permeate pressure losses (P_{pp}) and the pump suction pressure (P_{suc}), as shown below.

$$P_{hhp} = P_{avg} + NDP + \frac{\Delta P_{sys}}{2} + P_{pp} + P_{suc} \tag{24}$$

The high head pump power (Q_{hp}) is a function of the feed flowrate (F_m), the high head pump pressure rise (P_{hhp}), the high head pump efficiency (η_{hhp}) and the hydraulic pump coupling efficiency (η_{hpc}), as shown below.

$$Q_{hp} = \frac{F_m * 1000}{24 * 3600} * \frac{P_{hhp}}{\eta_{hhp} * \eta_{hpc} * 9866} \tag{25}$$

The seawater pumping power (Q_{spp}) depends on the feed flowrate (F_m), the seawater pump head (P_{sp}) and the seawater pump efficiency (η_{sp}), as below:

$$Q_{spp} = \frac{F_m * 1000}{24 * 3600} * \frac{P_{sp}}{\eta_{sp} * 9866} \tag{26}$$

Similarly, the booster pump power (Q_{bp}) is a function of the feed flowrate (F_m), the booster pump head (P_{bp}) and the booster pump efficiency (η_{bp}), as follows:

$$Q_{bp} = \frac{F_m * 1000}{24 * 3600} * \frac{P_{bp}}{\eta_{bp} * 9866} \tag{27}$$

Other power (Q_{op}) is a function of the plant capacity (PW_m) and the other specific power use (Q_{osp}), as below:

$$Q_{op} = \frac{PW_m * Q_{osp}}{24 * 1000} \tag{28}$$

The energy recovery (Q_{er}) depends on the recovery (R_m), the energy recovery efficiency (η_{er}) and the high head pump pressure (Q_{hp}), as follows:

$$Q_{er} = -(1 - R_m) * \eta_{er} * Q_{hp} \tag{29}$$

The total power use (Q_{tot}) is the sum of all previously mentioned powers, as follows:

Table 2
Required input parameters and output variables of the developed model.

Input Parameters	Output Variables		
	Thermal	Membrane	
Overall			
Capital and operating cost function parameters	T _{cr} TBT ΔT _{stage}	D _{flux} N _{flux} k _{agg}	β ^{therm} β ^{mem} α _t
Price of fuel to generate steam for heating (\$/MMBtu)	p _r c _b c _n	A NDP _n k _{fou}	τ ^{therm} τ ^{mem} T _{cp}
Cost of electricity (\$/kWh)		ΔP _{sys}	P _m R _{MED} R _{MSF}
F _{in} x _{c,F} ⁱⁿ T _F D _F		P _{pp} P _{suc} P _{sp} P _{bp} η _{hhp} η _{hpc} η _{sp} η _{bp} η _{er} Q _{osp}	

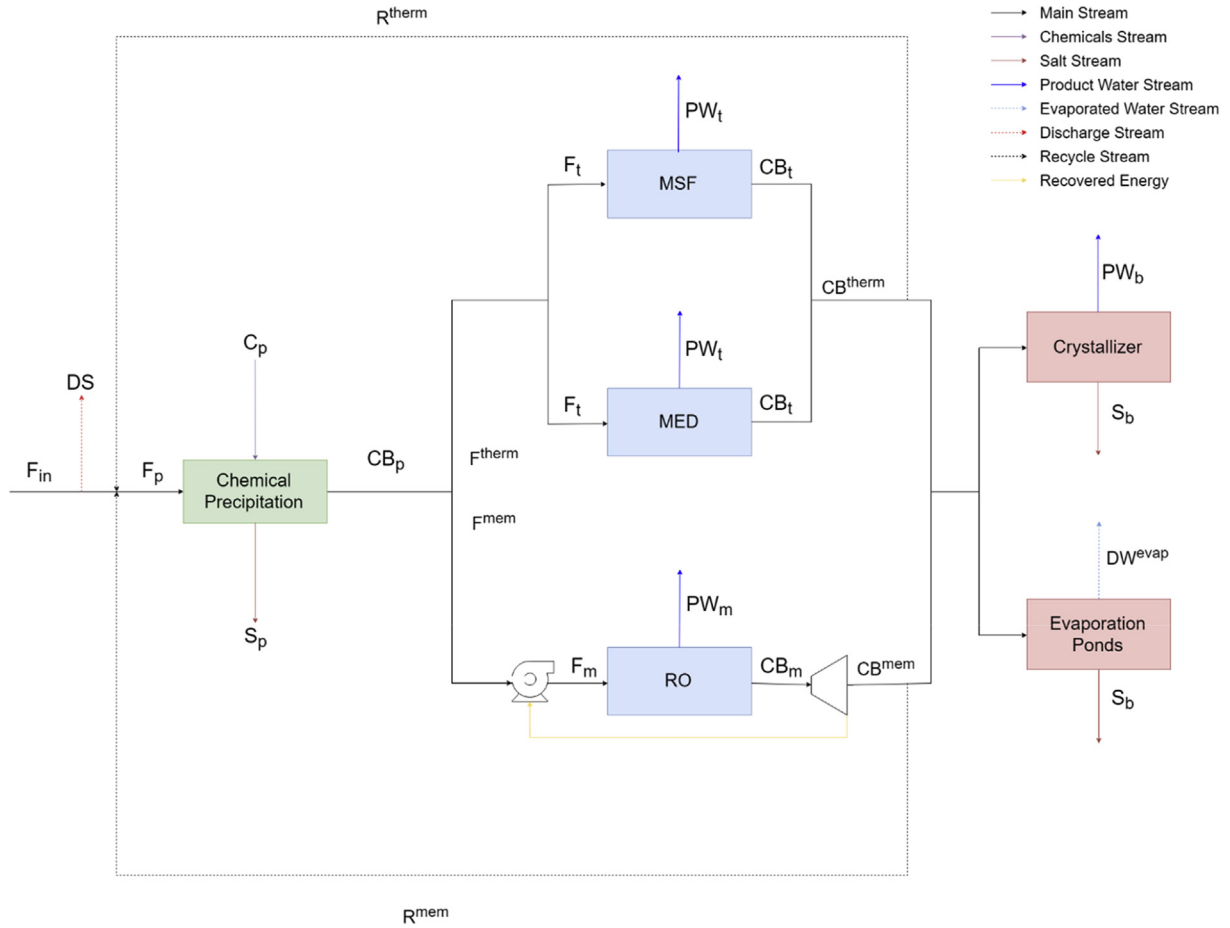


Fig. 1. Case study illustration.

$$Q_{tot} = Q_{hp} + Q_{spp} + Q_{bp} + Q_{om} + Q_{er} \quad (30)$$

2.1.5. Brine crystallizer

The brine crystallizer’s operating conditions were determined from SaltworksTech’s closed evaporator crystallizer (SaltWorksTech, n.d). The operating temperature (T_{crys}) is 90 °C, the maximum capacity is 125 m³/day and the recovery (R_{crys}) is 99%. Moreover, the estimated electrical energy consumption is 60 kWh/m³ product water. Thus, the operating costs were determined by calculating the amount of heat energy needed to raise the crystallizer feed temperature to 90 °C, in addition to the electrical energy consumption. As for the capital cost, the function developed by Mansour et al. (2018) was used.

2.2. Constraints

The implementation of new parameters in the model require the use of new constraints compared to the original model, in

Table 3 Technologies used in the case study model.

Chemical Processing	Thermal	Membrane	Brine-to-Salt
Lime Softening	MED MSF	RO	Evaporation Ponds Brine Crystallizer

addition to the adjustment of existing ones. The new constraints are shown in Table 1.

2.3. Objective function

The objective function remains the same as the model developed by Mansour et al. (2018) and it is to minimize the cost of the ZLD system design. It is the sum of the cost of the chemical processing technologies ($Cost^{chem}$), the cost of thermal technologies ($Cost^{therm}$), the cost of membrane technologies ($Cost^{mem}$) and the cost of the brine processing technologies ($Cost^{bp}$). The mathematical formulation is below.

$$Minimize \left(Cost^{chem} + Cost^{therm} + Cost^{mem} + Cost^{bp} \right) \quad (31)$$

The cost of each technology accounts for the capital and

Table 4 Feedwater composition used in this case study (Antar et al., 2012).

	Composition (mg/L)
Sodium ion [Na ⁺]	10,556
Calcium ion [Ca ²⁺]	400
Magnesium ion [Mg ²⁺]	1262
Potassium ion [K ⁺]	380
Sulfate [SO ₄ ²⁻]	2649
Chloride [Cl ⁻]	18,980
Bicarbonate [HCO ₃ ⁻]	140
TDS	34,367

Table 5
Case study assumptions.

Thermal	C_b	3.8 kJ/kgK	
	C_h	3.8 kJ/kgK	
	K_{GOR}	0.8	
	MED TBT	70 °C	
	MSF TBT	110 °C	
	n_r	3	
	T_{ac}	40 °C	
	T_{cr}	10 °C	
	ΔT_{stage}	2.5 °C	
	Membrane	A	3500
		D_{flux}	13.6 L/m ² h
		K_{agg}	1.05
		k_{fou}	0.8
NDP_n		28.2 bar	
N_{flux}		27.8 L/m ² h	
P_{bp}		3.3 bar	
P_{pp}		1 bar	
P_{sp}		1.7 bar	
P_{suc}		1 bar	
Q_{osp}		0.4 kWh/m ³	
ΔP_{sys}		2 bar	
η_{bp}		0.85	
η_{er}	0.95		
η_{hhp}	0.85		
η_{hpc}	0.97		
η_{sp}	0.85		
Crystallizer	R_{crys}	99%	
	T_{crys}	90 °C	
Energy Prices	Electricity (Germany)	0.17 \$/kWh	
	Electricity (KSA)	0.048 \$/kWh	
	Electricity (USA)	0.0665 \$/kWh	
	Gas (Europe)	5.88 \$/MMBtu	
	Gas (KSA)	1.25 \$/MMBtu	
	Gas (USA)	2.8 \$/MMBtu	

International Atomic Energy Agency (2013); SaltWorksTech, n.d.; US Energy Information Administration (2019); European Commission, 2018; International Energy Agency, 2018; Corbeau (2017); Saudi Electricity Company, 2018.

operating costs. The capital costs are power law functions in terms of the feed flowrate, the parameters of which, A and B, are taken from Mansour et al. (2018). As such, the pre-exponential factors for the capital costs of the chemical precipitation stage (A_p^{CAP}), thermal concentration stage (A_t^{CAP}), membrane concentration stage (A_m^{CAP}) and brine-to-salt processing stage (A_{bp}^{CAP}) are each multiplied by their corresponding inlet flowrate (F_p, F_t, F_m, F_{bp}), and raised to their respective exponent ($B_p^{CAP}, B_t^{CAP}, B_m^{CAP}, B_{bp}^{CAP}$).

Table 6
Total yearly costs (\$).

DF (%)	Total Cost	Capital Cost	Operating Cost
0	1,757,967	472,317	1,285,650
20	1,408,930	384,242	1,024,688
40	1,059,343	294,513	764,831
60	708,942	202,492	506,450
80	357,111	106,791	250,321
100	0	0	0

$$CAPEX^{chem} = (A_p^{CAP} F_p)^{B_p^{CAP}} \quad (32)$$

$$CAPEX^{therm} = (A_t^{CAP} F_t)^{B_t^{CAP}} \quad (33)$$

$$CAPEX^{mem} = (A_m^{CAP} F_m)^{B_m^{CAP}} \quad (34)$$

$$CAPEX^{bp} = (A_{bp}^{CAP} F_{bp})^{B_{bp}^{CAP}} \quad (35)$$

Furthermore, the operating costs of the chemical precipitation and the solar ponds technologies also follow a power law model, the parameters of which ($A_p^{OP}, B_p^{OP}, A_{SP}^{OP}, B_{SP}^{OP}$) are taken from Mansour et al. (2018).

$$OPEX^{chem} = (A_p^{OP} F_p)^{B_p^{OP}} \quad (36)$$

$$OPEX^{SP} = (A_{SP}^{OP} F_{SP})^{B_{SP}^{OP}} \quad (37)$$

Moreover, the operating costs of the remaining technologies (thermal, membrane and brine crystallizer) depend on their energy requirements in the form of heat and/or electricity. The heating costs (HC) are obtained by determining the cost of fuel needed to meet the steam requirements (US Department of Energy, 2012; Dieckmann et al., 2016). As for electricity costs (EC), they depend on the electricity requirements of the technologies and the price of 1 kW-hour (C_{elec}).

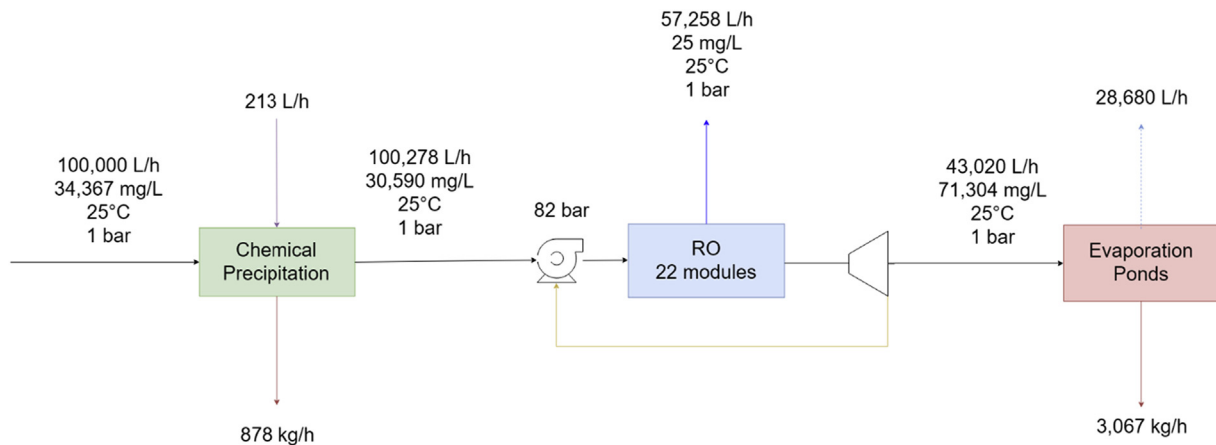


Fig. 2. The optimal configuration.

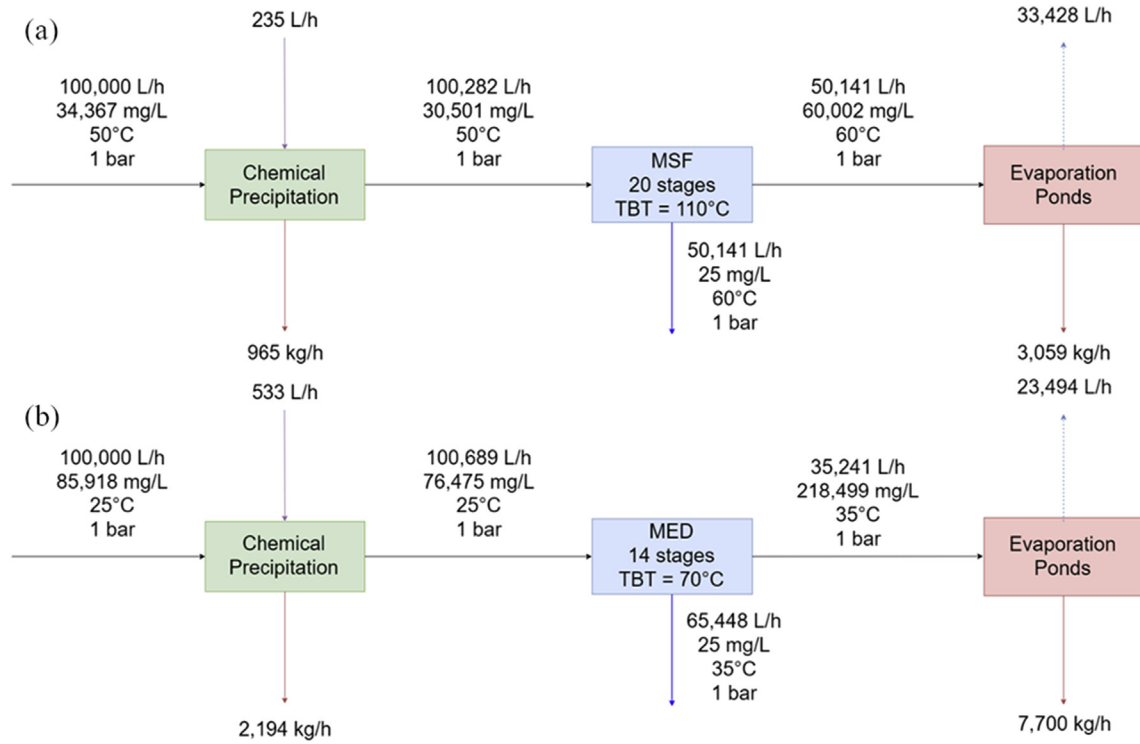


Fig. 3. Optimal ZLD system design for (a) temperature of 50 °C, (b) salinity of 85,918 mg/L.

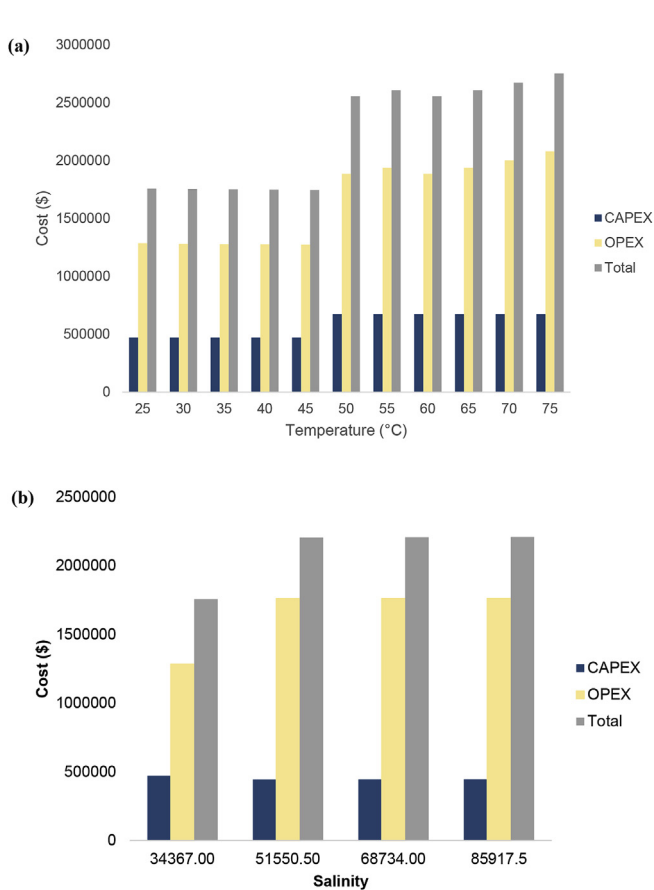


Fig. 4. Variation of capital, operating and total costs with: (a) the feed temperature, (b) the feed salinity.

$$HC^{therm} = \frac{Q_{ht} * 1000 * 24 * 3600 * 0.947817}{\eta_{combustion} * 10^6} * C_{gas} * 365 \quad (38)$$

$$HC^{crys} = \frac{Q_{hc} * 1000 * 24 * 3600 * 0.947817}{\eta_{combustion} * 10^6} * C_{gas} * 365 \quad (39)$$

$$EC^{mem} = (Q_{tot} * 24 * 1000) * C_{elec} * 365 \quad (40)$$

$$EC^{therm} = (Q_{et} * 24 * 1000) * C_{elec} * 365 \quad (41)$$

$$EC^{crys} = (Q_{crys} * 24 * 1000) * C_{elec} * 365 \quad (42)$$

$$OPEX^{mem} = EC^{mem} \quad (43)$$

$$OPEX^{therm} = HC^{therm} + EC^{therm} \quad (44)$$

$$OPEX^{crys} = HC^{crys} + EC^{crys} \quad (45)$$

As such, the total cost of each technology is the sum of its capital and operating costs.

$$Cost^{chem} = CAPEX^{chem} + OPEX^{chem} \quad (46)$$

$$Cost^{mem} = CAPEX^{mem} + OPEX^{mem} \quad (47)$$

$$Cost^{therm} = CAPEX^{therm} + OPEX^{therm} \quad (48)$$

$$Cost^{bp} = CAPEX^{bp} + OPEX^{bp} \quad (49)$$

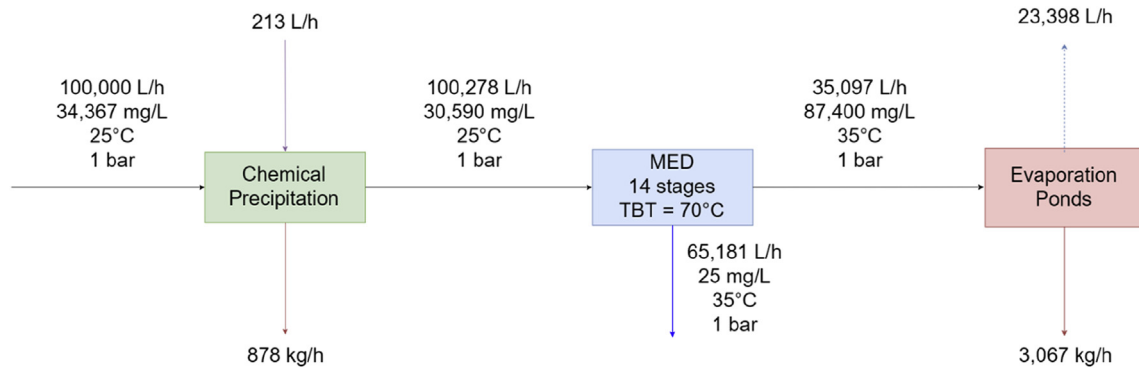


Fig. 5. Optimal ZLD system design for a theoretical electricity price of 0.77 \$/kWh (DF = 0%).

2.4. Problem implementation

This non-linear program (NLP) has been implemented using “What’sBest 16.0” LINDO Global Solver for Microsoft Excel 2016 on a notebook with Intel® Core™ i7-2670QM, 2.2 GHz, 8 GB RAM, 64-bit Operating System.

The required input parameters for running the model and the resulting output variables are listed in Table 2.

3. Case study

The ZLD network structure proposed for this work is shown in Fig. 1. Fresh brine, mixed with the recycled concentrated brine, enters the chemical processing stage where salt is produced and the generated concentrated brine is split between thermal (MED, MSF) and membrane technologies (RO). At the thermal and membrane stages, product water results from further concentrating the brine streams. Consequently, a fraction of the resulting concentrated brine streams is recycled and mixed with the main feed stream, while the remaining portion enters the brine-to-salt processing stage where more product water and salt are produced. The total dissolved solids (TDS) are assessed as one main “component” after the chemical processing stage given that the hardness is a subset of the TDS.

The technologies used in this case study are listed in Table 3. The feedwater composition is that of typical seawater, and it is shown in Table 4. The assumptions used for this case study are summarized in Table 5.

The aim of this case study is to show how the new model works and how it improves on the model developed by Mansour et al. (2018) in that it considers the effect of temperature, salinity and pressure. The user can set any value for any parameter and impose additional constraints that may apply to the system being considered. Thus, this case study is for illustrative purposes and may not exactly reflect a realistic scenario.

3.1. Results and discussion

The case study considers several discharge fractions to determine how the recommended ZLD scheme changes. Energy prices applicable in the USA have been utilized. A sensitivity analysis is conducted to observe how the scheme changes with different changes in the system, such as temperature, salinity and energy prices. The model is non-convex and the constraints are nonlinear. Therefore, all the solutions mentioned in this work are limited by the solver’s capabilities. Furthermore, the solver has a multi-start feature, which conducts the runs at different starting points. While this does not guarantee a global minimum, it does provide a

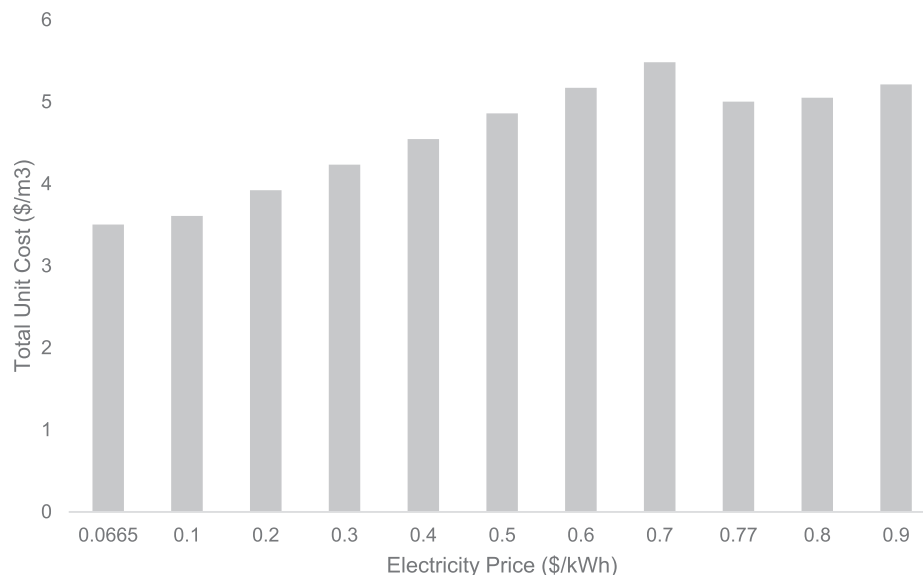


Fig. 6. Variation of the total unit cost with the electricity price (for USA gas prices).

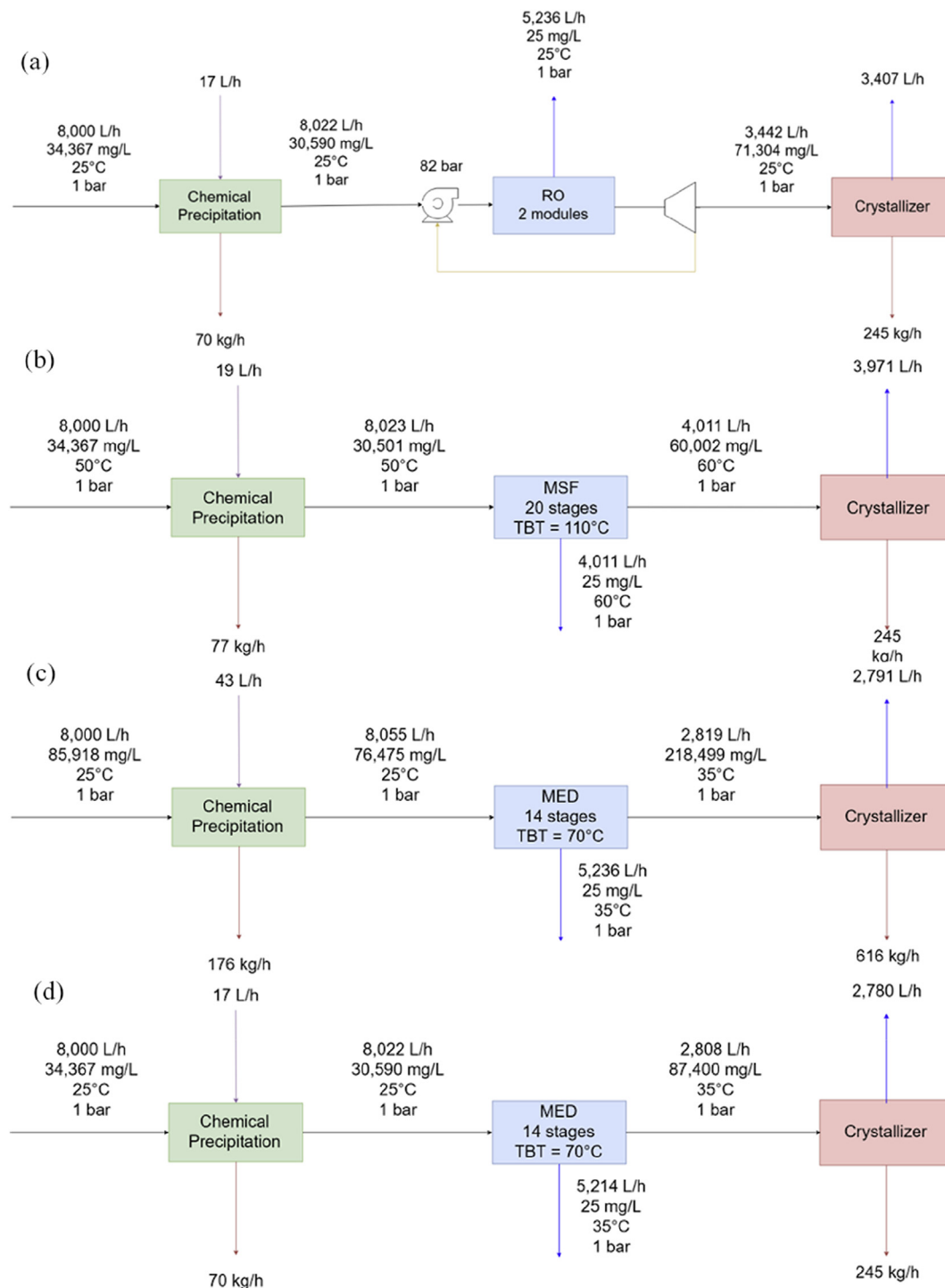


Fig. 7. Variation of capital, operating and total costs with the electricity price (for USA gas prices).

better confidence level for the solutions obtained.

3.1.1. Central optimization problem

The central optimization problem has been solved for various discharge fraction values ranging from 0 to 100% (Table S1 in the supplementary material). One configuration is obtained for all the discharge fraction values and consists of a lime softening unit, a reverse osmosis unit and evaporation ponds (Fig. 2).

It is interesting to note that the solver finds it optimal to run the

RO at the highest possible pressure, i.e. at the highest recovery, thus reducing the amount of concentrated brine going through the brine-to-salt processing stage, which is relatively more expensive in comparison. Moreover, for all the runs, solar ponds were chosen as the brine-to-salt processing technology because they are less expensive than the brine crystallizer and because no product water constraint was imposed. For comparison, and for a discharge fraction of 0%, selecting the MED instead of the RO would result in a 25.5% increase in the total cost (\$2,205,610), whereas selecting the

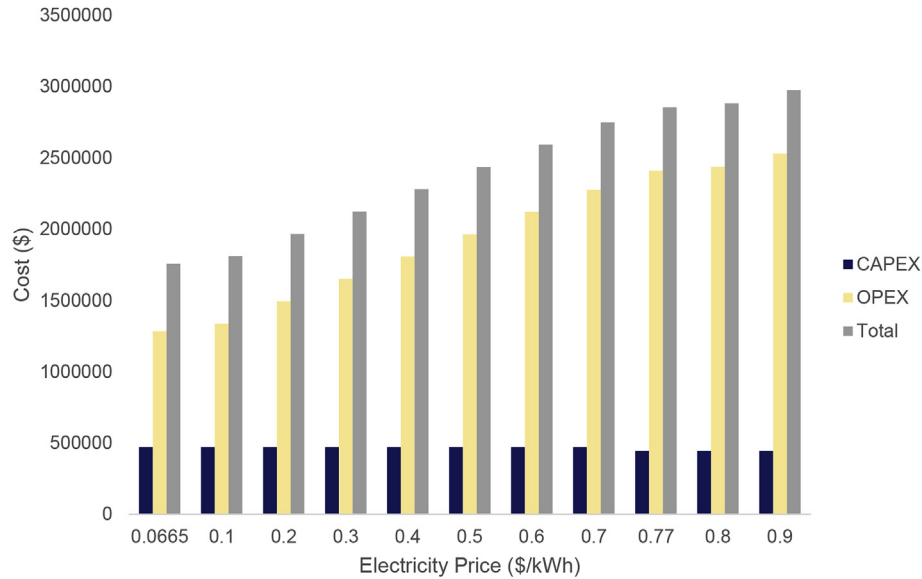


Fig. 8. Optimal ZLD system design with the solar ponds option removed (DF = 0%) for: (a) the standard case, (b) a feed temperature of 50 °C, (c) a feed salinity of 85,918 mg/L, (d) a theoretical electricity price of 0.11 \$/kWh.

MSF would result in a 36.2% increase in the price (\$2,394,768). In addition, selecting the brine crystallizer instead of solar ponds would result in a 139.47% increase in the total cost (\$4,109,822), mainly due to the crystallizer's energetic requirements and limited capacity, requiring multiple units in parallel. Therefore, the RO remains the cheapest brine concentration technology given that all its constraints are satisfied, and the solar ponds remain the cheapest brine-to-salt technology to use in the ZLD network. As expected, the higher the discharge fraction, the lower the cost as less feed is treated through the ZLD system, as seen in Table 6.

3.2. Sensitivity analysis

Several sensitivity analysis runs were conducted. The first set of runs was at different feed temperatures. The second set of runs looks into the effect of feed salinity, while the third investigates changes in energy prices. All the sensitivity runs are done at a discharge fraction of 0%.

3.2.1. Feed temperature sensitivity

The inlet feed temperature was varied between 25 and 75 °C. The resulting configuration (shown in Fig. 2) remains the same up to a temperature of 45 °C, which is the maximum temperature of operation for the RO membranes, after which the solver opts for thermal technologies (Fig. 3 (a)). Table S2 summarizes the obtained parameter values and the cost for 25 °C and 50 °C. The higher cost starting at 50 °C compared to the other values is due to the solver selecting the thermal technologies, which are more energy intensive. For feed temperatures of 50 °C and above, the MSF was chosen instead of the MED because it has a higher GOR, making it less costly. With the increase in the inlet temperature and the concomitant change in second stage technology from RO to MSF, the unit cost increases from 3.5 \$/m³ at 25 °C to reach 6.2 \$/m³ at 75 °C. Choosing the MED instead of the MSF would increase the cost by 36.3% (\$2,555,754 vs \$3,484,537) at 50 °C. The cost breakdown at each temperature is shown in Fig. 4 (a). For comparison purposes, adding a cooling stage before the RO unit was assessed. In this specific case, it was required to bring down the temperature of the feed from 50 °C to 45 °C, and the cooler-RO combination was found to be less costly than using a thermal unit, 4.3 \$/m³ vs 5.1 \$/m³,

respectively (Naguib and Gale, 2009).

3.2.2. Feed salinity sensitivity

For this set of sensitivity runs, different feed compositions are tested. The compositions are obtained by multiplying the original composition found in Table 4 by different values (i.e. multiplying all individual values by the same factor). The RO's salinity limit is determined by the pressure constraint previously mentioned, and was found to be about 72,000 mg/L. At high salinity values, the optimizer chooses thermal technologies instead of membrane technologies because membrane recovery is reduced significantly at higher salinity, meaning more brine will be processed, and thus a higher cost (Fig. 3 (b)). It is important to note that the brine concentration exiting the thermal concentration stage (218,499 mg/L) is not a limiting value. In fact, it is calculated through the design equations based on the thermal stage feed stream characteristics and assumptions used. From the thermal technologies, MED is selected over MSF because it is less costly. For example, at a feed salinity of 85,519 mg/L, MSF would lead to a 10.3% increase in the total cost compared to MED (\$2,437,146 vs \$2,209,624). Table S3 summarizes the obtained parameter values. It should be noted that the unit costs for salinities greater than 50,000 mg/L do not appear to vary by a great deal (3.85 \$/m³). Moreover, MED cost is not affected by feed salinity variation. The cost breakdown is shown in Fig. 4 (b).

3.2.3. Energy price sensitivity

Different energy prices based on different countries were considered for this set of sensitivity runs. In addition to the USA prices used in the original runs, sensitivity runs were conducted for energy prices in Germany and KSA. In all cases, the same configuration was obtained as that in Fig. 2, as the RO remains cheaper to use than the thermal technologies at these prices. Moreover, it was found that at the theoretical value of 0.77 \$/kWh (and above), the optimizer favors thermal technologies as they become cheaper in terms of total cost than the membrane option (for USA gas prices) as observed in Fig. 5. For the theoretical electricity price, selecting MSF instead of MED would cause an increase of 17.1% in the total cost (\$3,539,016 as opposed to \$3,022,839); hence, the MED is chosen. The parameter values are summarized in Table S4. The

Table 7
Comparison between old and new model.

	Mansour et al. (2018)	New Model
Input	<ul style="list-style-type: none"> • Feed flowrate: 500,000 L/h • Feed salinity: 12,000 mg/L • Chemical treatment, membrane, thermal and brine-to-salt processing options together with all associated performance parameters (fixed recovery and rejection) 	<ul style="list-style-type: none"> • Feed flowrate: 500,000 L/h • Feed salinity: 12,000 mg/L • Feed temperature: 25 °C • Feed Pressure: 1 bar • Energy Pricing: <ul style="list-style-type: none"> - Cost of Natural Gas: 2.8 \$/MMBTU - Electricity price: 0.0665 \$/kWh • Chemical treatment, membrane, thermal and brine-to-salt processing options together with all associated performance parameters
Output	<ul style="list-style-type: none"> • Chemical treatment, membrane, thermal and brine-to-salt processing technologies selected • Inlet and outlet flowrate (coming from and to) for each technology unit selected • Inlet and outlet salinity (coming from and to) for each technology unit selected • Capital & operating cost breakdown of the ZLD system (function of flowrate) 	<ul style="list-style-type: none"> • Chemical treatment, membrane, thermal and brine-to-salt processing technologies selected • Inlet and outlet flowrate (coming from and to) for each technology unit selected • Inlet and outlet salinity (coming from and to) for each technology unit selected • Inlet and outlet temperature (coming from and to) for each technology unit selected • Inlet and outlet pressure (coming from and to) for each technology unit selected • Number of stages required in each technology unit (if a staged design is selected) • Recovery of each brine concentration technology • Rejection of chemical precipitation and membrane technology • Capital & operating cost breakdown of the ZLD system (function of feed flowrate, temperature, pressure and salinity)
Technologies used	<ul style="list-style-type: none"> • Lime softening • Concentrator • SWRO • Solar Pond • Crystallizer 	<ul style="list-style-type: none"> • Lime softening • SWRO • Solar Pond
Cost comparison (\$/m ³ brine feed)	<p>Capital</p> <ul style="list-style-type: none"> • Chem: 0.03 • Therm: 0.03 • Mem: 0.19 • BP: 0.15 • Total: 0.40 <p>Operating</p> <ul style="list-style-type: none"> • Chem: 1.40 • Therm: 0.11 • Mem: 26.02 • BP: 0.04 • Total: 27.56 	<p>Capital</p> <ul style="list-style-type: none"> • Chem: 0.03 • Therm: 0.00 • Mem: 0.25 • BP: 0.07 • Total: 0.35 <p>Operating</p> <ul style="list-style-type: none"> • Chem: 1.35 • Therm: 0.00 • Mem: 0.14 • BP: 0.01 • Total: 1.51
CPU time	<ul style="list-style-type: none"> • Average runtime ranging between 20 and 60s 	<ul style="list-style-type: none"> • Average runtime ranging between 20 and 60s

variation of total unit cost with the electricity price and the cost breakdown are shown in Figs. 6 and 7, respectively.

3.2.4. No solar ponds

In all previous runs, the favored brine-to-salt processing technology was the solar ponds as they are cheaper, and no product water constraint is imposed. In this set of runs, the solar ponds option was removed in order to force the brine crystallizer option on the solver. The runs were done at different temperatures, salinity and at different energy prices. The inlet feed flowrate was decreased to 8000 L/h because of the capacity constraint of the crystallizer.

In all cases, the same results were obtained as in the previous sections, except that the brine crystallizer replaced the solar ponds in the final stage (Fig. 8 (a)). This means that for temperatures above 45 °C (Fig. 8 (b)), or for a feed salinity above 72,000 mg/L (Fig. 8(c)) or for USA electricity prices greater than 0.11\$/kWh (Fig. 8 (d)), the solver opts for thermal technologies. Table S5 summarizes the system parameters used for each case.

Hence, the inlet brine temperature, the inlet brine salinity as well as the electricity pricing all played a major role in the technology selection, between thermal and membrane options, within

the brine processing stage. It was found that membrane options were favored under relatively low temperature (ranging 25–45 °C), low salinity (ranging 34,367 - 72,000 mg/L), and low electricity pricing (ranging 0.048–0.76 \$/kWh for the solar ponds runs, 0.048–0.10 \$/kWh for the no solar ponds runs), whereas thermal options were favored for relatively higher temperature (above 45 °C), higher salinity (above 72,000 mg/L) and higher electricity pricing (above 0.76 \$/kWh for the solar ponds runs, 0.10 \$/kWh for the no solar ponds runs).

3.3. Model performance assessment

The model introduced by Mansour et al. (2018) proved to be very helpful in guiding the decision-making process of assembling cost-effective end-of-pipe ZLD systems, given an initial brine flowrate and salinity, as well as different treatment technologies to choose from. Mansour et al. (2018) captures all pertaining unit performance limitations in terms of flowrate and salinity. On the other hand, the model presented in this paper requires additional inlet information, mainly being brine inlet temperature and pressure conditions, as well as additional unit performance parameters. Furthermore, the model optimizes for the recoveries of the units,

which determines more accurately the optimal configuration of the ZLD system. Moreover, the presented model captures the effect of the temperature on the chemical precipitation stage, the membrane and thermal units. In addition, the corresponding energy requirements for each individual treatment unit can now be estimated more rigorously, by utilizing standard energy prices for predicting a major contribution of the operating cost portion that is associated with each generated design. For comparison purposes, the case studied by Mansour et al. (2018) was run with the new model and the differences between both models are presented in Table 7. The difference between the unit costs of both models is attributed to the fact that Mansour et al. (2018) rely on literature data to fit a model for the cost functions, whereas the new model uses the design equations of the technologies to predict the energy requirements and subsequently the cost.

4. Conclusion

This paper proposes an improvement on the model developed by Mansour et al. (2018) by accounting for temperature, salinity and pressure in selecting the optimal ZLD design. As such, the developed model can predict the energetic requirements of the system more accurately as well as the stream compositions, ensuring the optimal design for the system for a minimum amount of energy. Hence, this model allows for the design of cost-effective end-of-pipe ZLD systems making it a viable brine management strategy to reduce the environmental strain caused by brine disposal. The objective of the model is to minimize the cost of the system while respecting the imposed constraints. The model can be modified to accommodate new technologies or different types of technologies, given that their information is integrated in the model. This allows testing new and different combination of technologies that have not been tested yet. The model can also be altered so that it is able to select units in different arrangements (series or parallel). Moreover, the user can change parameters and impose different constraints to generate different scenarios. Hence, the proposed model can be for evaluating a proposed scheme's cost-effectiveness, under different conditions.

A case study was used to demonstrate how the model works. It should be noted that this model does not account for some feed characteristics, such as the presence of organic matter. Moreover, this model does not account for the effects of injecting antiscalant chemicals, which could slightly alter the composition of the feed, due to the very limited data available. Nonetheless, the model's flexibility and versatility render it suitable for any field requiring ZLD for the treatment of brine waste, given its ability to provide optimal cost-effective schemes. However, further investigations regarding how those different stream properties may further affect ZLD system design could perhaps be attempted, in case more data is found available in the near future.

Declaration of competing interest

The authors declare that they have no known competing financial interests or personal relationships that could have appeared to influence the work reported in this paper.

CRedit authorship contribution statement

Edgard El Cham: Investigation, Methodology, Software, Writing - original draft. **Sabla Alnouri:** Conceptualization, Funding acquisition, Supervision. **Fatima Mansour:** Writing - review & editing. **Mahmoud Al-Hindi:** Validation, Resources.

Acknowledgement

The authors would like to acknowledge the financial support received from the University Research Board (Award# 103187; Project# 23308) at the American University of Beirut.

Appendix A. Supplementary data

Supplementary data to this article can be found online at <https://doi.org/10.1016/j.jclepro.2019.119569>.

Nomenclature

A	membrane permeability constant
b	brine processing technology
A_b^{CAP}	constant of power function for capital cost equation of brine processing technology b \$/y
A_m^{CAP}	constant of power function for capital cost equation of membrane technology m \$/y
A_p^{CAP}	constant of power function for capital cost equation of chemical processing technology p \$/y
A_t^{CAP}	constant of power function for capital cost equation of thermal technology t \$/y
A_p^{OP}	constant of power function for operating cost equation of chemical processing technology p \$/y
A_{SP}^{OP}	constant of power function for operating cost equation of solar pond \$/y
BPE	boiling point elevation °C
B_b^{CAP}	exponent of power function for capital cost equation of brine processing technology b
B_m^{CAP}	exponent of power function for capital cost equation of membrane technology m
B_p^{CAP}	exponent of power function for capital cost equation of chemical processing technology p
B_t^{CAP}	exponent of power function for capital cost equation of thermal technology t
B_p^{OP}	exponent of power function for operating cost equation of chemical processing technology p
B_{SP}^{OP}	exponent of power function for operating cost equation of solar pond
c	component
C_{elec}	cost of electricity \$/kWh
C_{gas}	cost of natural gas \$/MMBtu
$CAPEX^{bp}$	brine processing technologies capital costs p \$/y
$CAPEX^{chem}$	chemical processing technologies capital costs \$/y
$CAPEX^{mem}$	membrane technologies capital costs \$/y
$CAPEX^{therm}$	thermal technologies capital costs \$/y
c_b	average brine specific heat capacity kJ/kgK
CB_m	flow of concentrated brine exiting a membrane technology m L/h
CB^{mem}	flow of the concentrated brine exiting all membrane technologies L/h
CB_p	flow of concentrated brine exiting a chemical processing p L/h
CB_t	flow of concentrated brine exiting a chemical processing technology p L/h
CB^{therm}	flow of concentrated brine exiting all thermal technologies L/h
c_h	specific heat in brine heater kJ/kgK
$Cost^{bp}$	cost of the brine processing technologies b \$/y
$Cost^{chem}$	cost of the chemical processing technologies p \$/y
$Cost^{mem}$	cost of the membrane technologies m \$/y
$Cost^{therm}$	cost of the thermal technologies t \$/y
C_p	flow of chemicals into chemical processing technology stream p L/h

DF	discharge fraction
D_{flux}	design average permeate flux L/m ² h
DS	discharge stream L/h
EC^{crys}	brine crystallizer electricity costs \$/y
EC^{mem}	membrane technologies electricity costs \$/y
EC^{therm}	thermal technologies electricity costs \$/y
F'_{in}	new inlet feed flow L/h
F_{in}	total inlet feed flow into system L/h
F_m	inlet feed flow into a membrane technology m L/h
F_p	inlet feed flow into a chemical processing technology p L/h
F_t	inlet feed flow into a thermal technology t L/h
F_{bp}	inlet feed flow into a brine processing technology bp L/h
GOR	gained output ratio
HC^{crys}	brine crystallizer heating costs \$/y
HC^{therm}	thermal technologies heating costs \$/y
k_{agg}	aggregation of the individual ions correction factor
k_{jou}	k_{GOR} fouling factor GOR equation parameter
k_{sal}	salinity correction factor
k_{tem}	temperature correction factor
m	membrane technology
n	number of stages
η_{bp}	booster pump efficiency
$\eta_{combustion}$	efficiency of combustion
η_{er}	energy recovery efficiency
η_{hhp}	high head pump efficiency
η_{hpc}	hydraulic pump coupling efficiency
η_{sp}	seawater pump efficiency
NDP	net driving pressure bar
NDP_n	nominal net driving pressure bar
N_{flux}	nominal permeate flux L/m ² h
$OPEX^{chem}$	chemical processing technologies operating costs \$/y
$OPEX^{crys}$	brine crystallizer operating costs \$/y
$OPEX^{mem}$	membrane technologies operating costs \$/y
$OPEX^{SP}$	solar pond operating costs \$/y
$OPEX^{therm}$	thermal technologies operating costs \$/y
p	chemical processing technology
P_{avg}	average pressure in membrane technology bar
P_{bp}	booster pump head bar
P_{hhp}	high head pump pressure rise bar
P_m	pressure of feed F_m into membrane technology m bar
P_{pp}	permeate pressure losses bar
P_{sp}	seawater pump head bar
P_{suc}	pump suction pressure bar
PW_b	flow of product water exiting a brine processing technology b L/h
PW_m	flow of product water exiting a membrane technology m L/h
PW_t	flow of product water exiting a thermal technology t L/h
Q_{bp}	booster pump power MW/d
Q_{crys}	required electricity for brine crystallizer MW/d
Q_{em}	total electrical power required for membrane technology m MW/d
Q_{er}	energy recovered MW/d
Q_{et}	required electricity for thermal technology t MW/d
Q_{hc}	required heat energy for brine crystallizer MW/d
Q_{hhp}	high head pump power MW/d
Q_{ht}	required heat energy for thermal technology t MW/d
Q_{op}	other power MW/d
Q_{osp}	specific other power use kWh/m ³
Q_{spp}	seawater pumping power MW/d
Q_{sp}	specific power use kWh/m ³ product water
Q_{tot}	total power use MW/d
R_m	recovery of membrane technology m

R^{mem}	portion of membrane concentrated brine (CB ^{mem}) that is recycled to the beginning of system L/h
R_t	recovery of thermal technology t
R^{therm}	portion of thermal concentrated brine (CB ^{therm}) that is recycled to the beginning of system L/h
S_b	amount of salt produced by a brine processing technology b kg/h
S_p	amount of salt produced by a chemical processing technology p kg/h
t	thermal technology
T_{ac}	average condensing temperature °C
T_{bh}	brine heater temperature rise °C
TBT	top brine temperature °C
T_{cp}	temperature of the chemical precipitation stage °C
T_{cr}	distillation plant condenser range °C

References

- Able, C.M., Ogden, D.D., Tremblay, J.P., 2018. Sustainable management of hypersaline brine waste: zero liquid discharge via Joule-heating at supercritical condition. *Desalination* 444, 84–93.
- Ahirrao, S., 2014. Chapter 13 - zero liquid discharge solutions. In: Ranade, V.V., Bhandari, V.M. (Eds.), *Industrial Wastewater Treatment, Recycling and Reuse*. Butterworth-Heinemann, Oxford, pp. 489–520.
- Al-Karaghoul, A., Kazmerski, L.L., 2013. Energy consumption and water production cost of conventional and renewable energy powered desalination processes. *Renew. Sustain. Energy Rev.* 24, 343–356.
- Antar, M., Lienhard, J.H., Smith, A., Blanco, J., Zaragoza, G., 2012. Solar Desalination. Baghdad, Y.N., Alnouri, S.Y., Matsuura, T., Tarboush, B.J.A., 2018. Temperature effects on concentration polarization thickness in thin-film composite reverse osmosis membranes. *Chem. Eng. Technol.* 41, 1905–1912.
- Corbeau, A.-S., 2017. Regional Gas Industry Issues and Opportunities. King Abdullah Petroleum Studies and Research Center.
- Dieckmann, S., Krishnamoorthy, G., Aboumadi, M., Pandian, Y., Dersch, J., Krüger, D., Al-Rasheed, A.S., Krüger, J., Ottenburger, U., 2016. Integration of solar process heat into an existing thermal desalination plant in Qatar. *AIP Conf. Proc.* 1734 (1), 140001.
- Eltawil, M.A., Zhengming, Z., Yuan, L., 2009. A review of renewable energy technologies integrated with desalination systems. *Renew. Sustain. Energy Rev.* 13 (9), 2245–2262.
- European Commission, 2018. Electricity Price Statistics. European Union.
- Frantz, C., Seifert, B., 2015. Thermal analysis of a multi effect distillation plant powered by a solar tower plant. *Energy Procedia* 69, 1928–1937.
- Gilron, J., 2016. Chapter 12 - brine treatment and high recovery desalination. In: Hankins, N.P., Singh, R. (Eds.), *Emerging Membrane Technology for Sustainable Water Treatment*. Elsevier, Boston, pp. 297–324.
- Giwa, A., Dufour, V., Al Marzooqi, F., Al Kaabi, M., Hasan, S.W., 2017. Brine management methods: recent innovations and current status. *Desalination* 407, 1–23.
- Gude, V.G., 2018. Exergy evaluation of desalination processes. *ChemEngineering* 2, 28.
- International Atomic Energy Agency, 2013. DEEP 5 User Manual.
- International Energy Agency, 2018. Natural Gas Information: Overview, 2018 edition.
- Jones, E., Qadir, M., van Vliet, M.T.H., Smakhtin, V., Kang, S.-m., 2019. The state of desalination and brine production: a global outlook. *Sci. Total Environ.* 657, 1343–1356.
- Kucera, J., 2015. *Reverse Osmosis: Industrial Processes and Applications*. Wiley, Hoboken, NJ.
- Lee, S., Choi, J., Park, Y.-G., Shon, H., Ahn, C.H., Kim, S.-H., 2019. Hybrid desalination processes for beneficial use of reverse osmosis brine: current status and future prospects. *Desalination* 454, 104–111.
- Liu, T.-K., Weng, T.-H., Sheu, H.-Y., 2018. Exploring the environmental impact assessment commissioners' perspectives on the development of the seawater desalination project. *Desalination* 428, 108–115.
- Loganathan, K., Chelme-Ayala, P., Gamal El-Din, M., 2016. Pilot-scale study on the treatment of basal aquifer water using ultrafiltration, reverse osmosis and evaporation/crystallization to achieve zero-liquid discharge. *J. Environ. Manag.* 165, 213–223.
- Lopez, D.E., Tremblay, J.P., 2017. Desalination of hypersaline brines with joule-heating and chemical pre-treatment: conceptual design and economics. *Desalination* 415, 49–57.
- Lu, K.J., Cheng, Z.L., Chang, J., Luo, L., Chung, T.-S., 2019. Design of zero liquid discharge desalination (ZLDD) systems consisting of freeze desalination, membrane distillation, and crystallization powered by green energies. *Desalination* 458, 66–75.
- Mackey, E.D., Seacord, T., 2008. *Regional Solutions for Concentrate Management*. Water ReUse Foundation, Alexandria, VA.
- Mansour, F., Alnouri, S.Y., Al-Hindi, M., Azizi, F., Linke, P., 2018. Screening and cost

- assessment strategies for end-of-Pipe Zero Liquid Discharge systems. *J. Clean. Prod.* 179, 460–477.
- Mickley, M., 2008. Survey of High-Recovery and Zero Liquid Discharge Technologies for Water Utilities. WaterReuse Foundation, Alexandria, VA.
- Morillo, J., Usero, J., Rosado, D., El Bakouri, H., Riaza, A., Bernaola, F.-J., 2014. Comparative study of brine management technologies for desalination plants. *Desalination* 336, 32–49.
- Naguib, Ramez, 2009. Total cost of ownership: for air-cooled and water-cooled chiller systems. *ASHRAE J.* 51 (4), 42+. Gale Academic Onefile, Accessed 4 Nov. 2019.
- Onishi, V.C., Ruiz-Femenia, R., Salcedo-Díaz, R., Carrero-Parreño, A., Reyes-Labarta, J.A., Fraga, E.S., Caballero, J.A., 2017. Process optimization for zero-liquid discharge desalination of shale gas flowback water under uncertainty. *J. Clean. Prod.* 164, 1219–1238.
- Pérez-Gonzalez, A., Urriaga, A.M., Ibañez, R., Ortiz, I., 2012. State of the art and review on the treatment technologies of water reverse osmosis concentrates. *Water Res.* 46, 267–283.
- SaltWorksTech, SaltMaker-MultiEffect Closed Evaporator Crystallizer.
- Saudi Electricity Company, 2018. Consumption tariffs. <https://www.se.com.sa/en-us/customers/Pages/TariffRates.aspx>.
- Schwantes, R., Chavan, K., Winter, D., Felsmann, C., Pfaffert, J., 2018. Techno-economic comparison of membrane distillation and MVC in a zero liquid discharge application. *Desalination* 428, 50–68.
- Subramani, A., Jacangelo, J.G., 2014. Treatment technologies for reverse osmosis concentrate volume minimization: a review. *Separ. Purif. Technol.* 122, 472–489.
- Tillberg, F., 2004. ZLD-systems an Overview. Department of Energy Technology. Royal Institute of Technology, Stockholm.
- Tong, T., Elimelech, M., 2016. The Global Rise of Zero Liquid Discharge for Wastewater Management: Drivers, Technologies, and Future Directions.
- Tsai, J.-H., Macedonio, F., Drioli, E., Giorno, L., Chou, C.-Y., Hu, F.-C., Li, C.-L., Chuang, C.-J., Tung, K.-L., 2017. Membrane-based zero liquid discharge: myth or reality? *J. Taiwan Inst. Chem. Eng.* 80, 192–202.
- Tufa, Ramato A., Curcio, E., Brauns, E., Van Baak, W., Fontananova, E., Di Profio, G., 2015. Membrane distillation and reverse electrodialysis for near-zero liquid discharge and low energy seawater desalination. *J. Membr. Sci.* 496, 325–333.
- US Department of Energy, 2012. Benchmark the fuel cost of steam generation. https://www.energy.gov/sites/prod/files/2014/05/f16/steam15_benchmark.pdf.
- US Energy Information Administration, 2019a. Electric power monthly. https://www.eia.gov/electricity/monthly/current_month/epm.pdf.
- US Energy Information Administration, 2019b. Natural Gas Weekly Update. US Department of Energy.